Performance Analysis of Brushless DC Motors Including Features of the Control Loop in the Finite Element Modeling

S. L. Ho, W. N. Fu, H. L. Li, H. C. Wong, and H. Tan

Abstract—**A time stepping finite element model for analyzing the performance of brushless d.c. motors is presented. The control loop is coupled into the system equations. The eddy-currents in the permanent magnets (PM) are also taken into account in the proposed circuit-field coupled method. By representing the PM as a "squirrel cage" then the eddy-current loss in the PM can be estimated. The model can directly take care of the nonsinusoidal quantities of the supplied voltages, the phase currents and the magnetic fields.**

Index Terms—**Brushless d.c. motor, control, eddy-current, finite element.**

I. INTRODUCTION

IN BRUSHLESS d.c. motors, the terminal stator voltages of each phase are controlled by power electronic switches. The impressed voltages comprise of a series of pulses of varying widths and the stator phase currents are essentially nonsinusoidal. High order harmonics in the currents and in the magnetic fields will have significant effects upon the motor output torque and corresponding performances. Moreover, the eddy-current in the permanent magnet (PM) is usually neglected, and this is acceptable for ferrite magnets because their conductivity is very small. However, for motors with rare-earth magnets whose conductivity is much higher (typically between 0.7 and 1.1 $\times$ $10^6/\Omega$m), then the eddy-current loss in such PM is comparable to the normal iron losses of conventional motors [1]–[3]. Since the temperature-rise will greatly affect the performance of PM materials, it is desirable to evaluate the eddy current loss in the PM. Although many researchers have studied the performances of brushless d.c. motors using finite element methods (FEM), most methods still cannot take into account the features of the control loop into the computation [4], [5]. On the other hand, in the normal 2-D FEM method, the eddy-current in the PM can be included simply by adding the $\sigma\partial A/\partial t$ term into the curl–curl diffusion equation [6]. This means the motor is assumed to have an infinite axial length. Consequently, this assumption is suitable when one studies the cross-sectional magnetic field distribution of the motor, but it will introduce additional errors when computing the eddy-current loss, since it is difficult to ensure the eddy-current could form a complete loop within the PM material being considered.

In this paper a time stepping FEM model is introduced to simulate the operation of brushless d.c. motors. The control loop is coupled to the voltage driven FEM of the motor and hence the stator windings could be fed with the actual output voltages from the converter. In order to include the eddy-current in the 2-D FEM, the circuit-field coupled multi-slice method for modeling the squirrel rotor cage of induction motor [7] is extended to cover PM motors as well. Since the eddy-currents flow mainly in the axial direction, a PM is divided into several "conductor bars" and they are inter-connected together by resistances. The circuit equations of these conductors are coupled with the multi-slice FEM and the current densities in the PM can be computed directly.

The simulation programs consist of two model blocks: the circuit-field-torque coupled FEM model and the control loop model. In the FEM model the inputs are the stator phase voltages and the load torque, whereas the outputs are the stator phase currents, rotor position and rotor speed. In the control loop model the voltage applied to the terminals of the stator windings of the motor is determined according to the control strategy and the power electronic switching circuits. A three-phase winding PM brushless d.c. motor system is used as a typical example to demonstrate usefulness of the proposed algorithm.

II. CIRCUIT-FIELD-TORQUE COUPLE FEM MODEL

A. Dealing With Eddy-Current in PM

Here the PM is divided into N bars and the motor is divided into M slices (Fig. 1). With the magnetization vector method, the excitation from the PM can be described by its remanent flux density B_r and equivalent reluctivity ν. The Maxwell's equations applied to the domain in the nth bar of the mth slice will give rise to the following Poisson equation:

$$\nabla \times (\nu\nabla \times A) + \sigma\frac{\partial A}{\partial t} - \frac{\sigma}{l_M} u_{mn} = \nabla \times (\nu B_r) \quad (1)$$

where

A is the axial component of the magnetic vector potential,
ν is the reluctivity of the material,
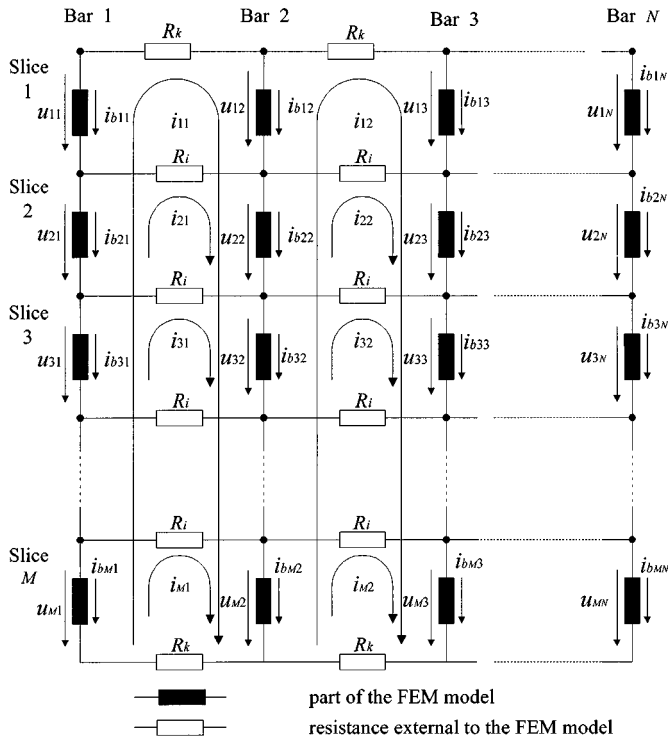σ is the conductivity of the material,

Fig. 1. Equivalent circuit for a PM.

u_{mm} is the voltage between the two terminals of the nth bar on the mth slice, and

$l_M = l/M$ and l is the axial length of the iron core.

The total current in the nth bar of the mth slice is:

$$i_{bmn} = \sigma \left(\iint\limits_{\Omega_{mn}} \left(-\frac{\partial A}{\partial t} + \frac{u_{mn}}{l_M} \right) d\Omega \right). \quad (2)$$

A network for representing the PM is shown in Fig. 1. Two adjacent bars are connected by the end resistor R_k at the two ends as well as by the inter-bar resistor R_i along the axial length of the motor. For a network of the PM having M slices and N bars, one could trace the loops for the mesh-currents in the clockwise direction and use the $M \times (N-1)$ mesh currents (labeled $i_{m1}, i_{m2}, \ldots, i_{m(N-1)}, m = 1, \ldots, M$) to describe the circuits as shown in Fig. 1. The branch currents of the bars can be expressed as:

$$\begin{bmatrix} i_{bm1} \\ i_{bm2} \\ i_{bm3} \\ \vdots \\ i_{bmN} \end{bmatrix} = - \begin{bmatrix} 1 & 0 & 0 & & 0 \\ -1 & 1 & 0 & & 0 \\ 0 & -1 & 1 & \cdots & 0 \\ & & \vdots & \ddots & \\ 0 & 0 & 0 & & -1 \end{bmatrix} \begin{bmatrix} i_{11} \\ i_{12} \\ i_{13} \\ \vdots \\ i_{1(N-1)} \end{bmatrix}$$

$$- K \begin{bmatrix} 1 & 0 & 0 & & 0 \\ -1 & 1 & 0 & & 0 \\ 0 & -1 & 1 & \cdots & 0 \\ & & \vdots & \ddots & \\ 0 & 0 & 0 & & -1 \end{bmatrix} \begin{bmatrix} i_{m1} \\ i_{m2} \\ i_{m3} \\ \vdots \\ i_{m(N-1)} \end{bmatrix}. \quad (3)$$

where $i_{m1}, i_{m2}, \ldots, i_{m(N-1)}, (m = 1, \ldots, M)$ are the mesh currents. When $m = 1$, $K = 0$. For $m > 1$, $K = 1$. Substituting (3) into (2) one obtains the branch equations as:

$$\sigma \left(\iint\limits_{\Omega_{mn}} \left(-\frac{\partial A}{\partial t} + \frac{u_{mn}}{l_M} \right) d\Omega \right)$$

$$+ \begin{bmatrix} 1 & 0 & 0 & & 0 \\ -1 & 1 & 0 & & 0 \\ 0 & -1 & 1 & \cdots & 0 \\ & & \vdots & \ddots & \\ 0 & 0 & 0 & & -1 \end{bmatrix} \begin{bmatrix} i_{11} \\ i_{12} \\ i_{13} \\ \vdots \\ i_{1(N-1)} \end{bmatrix}$$

$$+ K \begin{bmatrix} 1 & 0 & 0 & & 0 \\ -1 & 1 & 0 & & 0 \\ 0 & -1 & 1 & \cdots & 0 \\ & & \vdots & \ddots & \\ 0 & 0 & 0 & & -1 \end{bmatrix} \begin{bmatrix} i_{m1} \\ i_{m2} \\ i_{m3} \\ \vdots \\ i_{m(N-1)} \end{bmatrix} = 0 \quad (4)$$

where $m = 1, 2, \ldots, M$ and $n = 1, 2, \ldots N$. There are totally $M \times N$ branch equations. The total number of $M \times (N-1)$ mesh-current equations can be further established. For the loop $i_{11}, i_{12}, \ldots, i_{1(N-1)}$:

$$\sum_{m=1}^{M} \begin{bmatrix} 1 & -1 & 0 & \cdots & 0 \\ 0 & 1 & -1 & \cdots & 0 \\ 0 & 0 & 1 & \cdots & 0 \\ \vdots & \vdots & \vdots & \ddots & \vdots \\ 0 & 0 & 0 & \cdots & -1 \end{bmatrix} \begin{bmatrix} u_{m1} \\ u_{m2} \\ \vdots \\ u_{mN} \end{bmatrix} + (-2R_k)I$$

$$\cdot \begin{bmatrix} i_{11} \\ i_{12} \\ \vdots \\ i_{1(N-1)} \end{bmatrix} + (-R_k)I \begin{bmatrix} i_{M1} \\ i_{M2} \\ \vdots \\ i_{M(N-1)} \end{bmatrix} = 0 \quad (5)$$

where I is a unit diagonal matrix. For the loop $i_{m1}, i_{m2}, \ldots, i_{m(N-1)}$ $(m = 2, \ldots, M-1)$:

$$\begin{bmatrix} 1 & -1 & 0 & \cdots & 0 \\ 0 & 1 & -1 & \cdots & 0 \\ 0 & 0 & 1 & \cdots & 0 \\ \vdots & \vdots & \vdots & \ddots & \vdots \\ 0 & 0 & 0 & \cdots & -1 \end{bmatrix} \begin{bmatrix} u_{m1} \\ u_{m2} \\ \vdots \\ u_{m(N-1)} \end{bmatrix}$$

$$+ KR_iI \begin{bmatrix} i_{(m-1)1} \\ i_{(m-1)2} \\ \vdots \\ i_{(m-1)(N-1)} \end{bmatrix} + (-2R_i)I$$

$$\cdot \begin{bmatrix} i_{m1} \\ i_{m2} \\ \vdots \\ i_{m(N-1)} \end{bmatrix} + R_iI \begin{bmatrix} i_{(m+1)1} \\ i_{(m+1)2} \\ \vdots \\ i_{(m+1)(N-1)} \end{bmatrix} = 0. \quad (6)$$

When $m = 2$, $K = 0$. If $m > 2$, then $K = 1$. For the loop $i_{M1}, i_{M2}, \ldots, i_{M(N-1)}$:

$$
\begin{bmatrix}
1 & -1 & 0 & \cdots & 0 \\
0 & 1 & -1 & \cdots & 0 \\
0 & 0 & 1 & \cdots & 0 \\
\vdots & \vdots & \vdots & \ddots & \vdots \\
0 & 0 & 0 & \cdots & -1
\end{bmatrix}
\begin{bmatrix}
u_{M1} \\
u_{M2} \\
\vdots \\
u_{M(N-1)}
\end{bmatrix}
$$

$$
+ (-R_k)\mathbf{I}
\begin{bmatrix}
i_{11} \\
i_{12} \\
\vdots \\
i_{1(N-1)}
\end{bmatrix}
+ R_i\mathbf{I}
\begin{bmatrix}
i_{(M-1)1} \\
i_{(M-1)2} \\
\vdots \\
i_{(M-1)(N-1)}
\end{bmatrix}
$$

$$
+ (-R_k - R_i)\mathbf{I}
\begin{bmatrix}
i_{M1} \\
i_{M2} \\
\vdots \\
i_{M(N-1)}
\end{bmatrix}
= 0. \tag{7}
$$

The magnetic field equation (1) together with the branch equation (4) and the mesh-current equations (5)–(7), will give rise to the basic governing formulas in the PM domain.

B. Basic Equations in Other Domains

In the stator conductor domain, the field equation is:

$$
\nabla \times (\nu \nabla \times A) - (i_s/S) = 0 \tag{8}
$$

where i_s is the stator phase current and S is the total cross-sectional area of one turn on one coil side (parallel branches are considered as one turn). The stator circuit equation of one phase is:

$$
\frac{l_M N_{\phi 1} \sum_{m=1}^{M} \left(\iint_{\Omega_m^+} \frac{\partial A}{\partial t} d\Omega - \iint_{\Omega_m^-} \frac{\partial A}{\partial t} d\Omega \right)}{\sum_{m=1}^{M} \iint_{\Omega_m^+ + \Omega_m^-} d\Omega}
$$

$$
+ R_1 i_s + L_\sigma \frac{di_s}{dt} = u_s \tag{9}
$$

where
- R_1 is the total stator resistance of one phase winding,
- L_σ is the leakage inductance of the end windings,
- $N_{\phi 1}$ is the total number of serial connected conductors per phase,
- u_s is the applied voltage on the stator phase, and
- Ω^+ and Ω^- are, respectively, the cross-sectional areas of the "go" and "return" side of the phase conductors of the coils.

The field equation in the iron domains and in the air-gap is

$$
\nabla \times (\nu \nabla \times A) = 0. \tag{10}
$$

C. Global System Equations

The FEM equations together with the stator circuit equations and the torque balance equation will give rise to the large nonlinear equations of the system. The unknowns are, respectively, the magnetic vector potentials, the currents in the stator windings, the voltage of the bars (PM domain) on each slice, the mesh-current in the PM network, the rotor speed and the rotor position. The input excitations are the stator voltages and the remanent flux density B_r in the PM domain. The Backward Euler's method is used to discretize the time variable. The set of system equations is solved by the sub-block method [8]. When the magnetic field distribution and current as well as their changing against time are known, the eddy-current loss and iron loss can be computed directly [9].

III. SIMULATION OF THE CONTROL LOOP

The impressed terminal voltages are determined by the controller. In the control loop simulation, the inputs are either the speed reference or the current reference. The feedback signals are the stator phase currents, the rotor position and the rotor speed. The outputs are the stator phase voltages.

A. Current Hysteresis Control

The magnitude of the current reference I_s^* can be input or determined by the proportional and integral (PI) controller of the speed loop from:

$$
I_s^* = \begin{cases}
K_p(\omega^* - \omega) + I_{I(k)}^* & -I_{\max} \le I_s^* \le I_{\max} \\
I_{\max} & I_s^* > I_{\max} \\
-I_{\max} & I_s^* < -I_{\max}.
\end{cases} \tag{11}
$$

where $I_{I(k)}^*$ is

$$
\begin{cases}
I_{I(0)}^* = 0 \\
I_{I(k)}^* = I_{I(k-1)}^* + \dfrac{\omega^* - \omega}{T_s} \Delta T.
\end{cases} \tag{12}
$$

In (11) and (12), ω^* is the reference value of the input rotor speed; ω is the rotor speed feedback from the motor; K_p and T_s are, respectively, the proportionality factor and the integral factor; ΔT is the step size and $I_{\max}$ is the maximum allowable value of the stator current. The current reference is:

$$
i_s^* = I_s^* i^* \tag{13}
$$

where i^* is the expected current waveform but with unit magnitude. The stator voltage is controlled by the following current hysteresis loop when $i_s^* \ne 0$:

$$
u_{s(k)} = \begin{cases}
+U_D & i_s < i_s^* - \Delta i \\
-U_D & i_s > i_s^* + \Delta i \\
u_{s(k-1)} & i_s^* - \Delta i \le i_s \le i_s^* + \Delta i
\end{cases} \tag{14}
$$

where U_D is the magnitude of the voltage output from the converter (Fig. 2) and $2\Delta i$ is the width of the control band. When $i_s^* = 0$, the associated circuit will be open-circuited. When one of the stator windings is open-circuited, e.g., $i_A = 0$, then this additional constraint should be included in the system equations
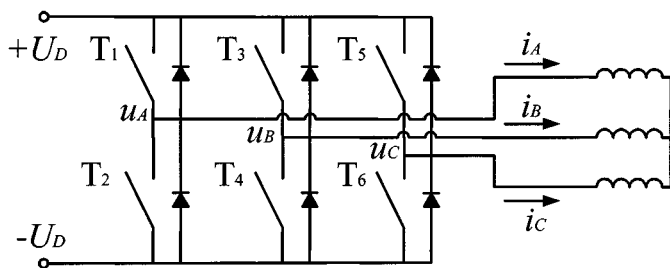
Fig. 2.   Representation of the switching elements.

TABLE I
REPRESENTATION OF THE FREE WHEELING DIODES

		Before switching off	After switching off	
			When $|i_A| \neq 0$	After $|i_A|$ reaches zero
If	$i_A > 0$		$u_A = -U_D$	Open circuit
If	$i_A < 0$		$u_A = +U_D$	Open circuit

in a manner which is similar to that commonly used in dealing with homogeneous boundary conditions in FEM analysis.

When the motor currents are controlled with a hysteresis-regulator, usually the switching period is smaller than the step size of the time stepping method. If the currents change quickly, the computed currents will not fall within the hysteresis band and a large error will appear. In such case the step size will be automatically reduced to half of its original value.

B. PWM Voltage Control

The stator phase current can also be controlled by changing the values of the voltages applied to the terminals of the stator windings by the PI method. The changes in the voltages are implemented by using pulse-width modulation (PWM). The time period of the PWM carrier is usually smaller than the time stepping size. The average stator voltage during the stepping period is used as the input voltage in the FEM. Thus if the effect of the very high-order harmonics can be ignored, it is not necessary to use very small step size and the computing time can be reduced significantly.

C. Effect of Diodes in Parallel With the Switch Elements

The electronic switch is simply taken as an ideal switch. When it is turned on it is short-circuited, while if it is turned off it is open circuited. The effect of the free wheeling diodes connected in parallel with the switch elements is included in the modeling of the switch elements. For example, before the switch T_1 is turned off, the phase current i_A is positive (Fig. 2). By the time when the switch T_1 is turned off, i_A will not suddenly fall to zero due to the inductance in the circuit. Actually it will continue to flow through the diode connected in parallel with T_2. Therefore u_A is equal to $-U_D$ during this time period. When i_A decreases to zero, then phase A will be open-circuited. The effect of the free wheeling diode upon phase A is summarized as in Table I.
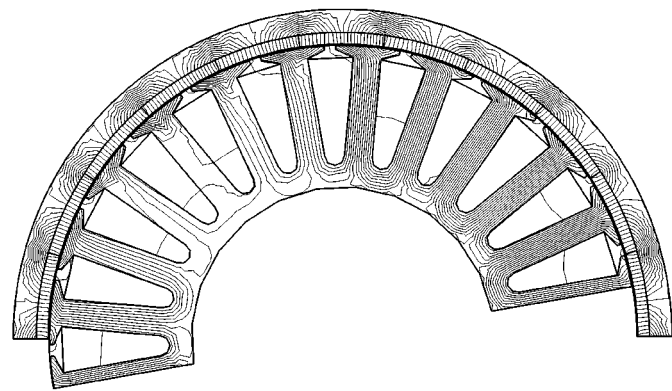

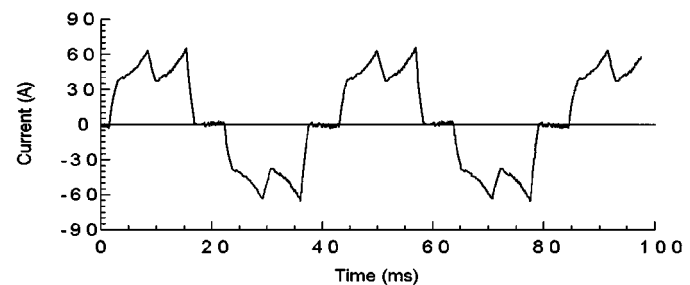Fig. 3.   Computed flux distribution at steady-state operation.

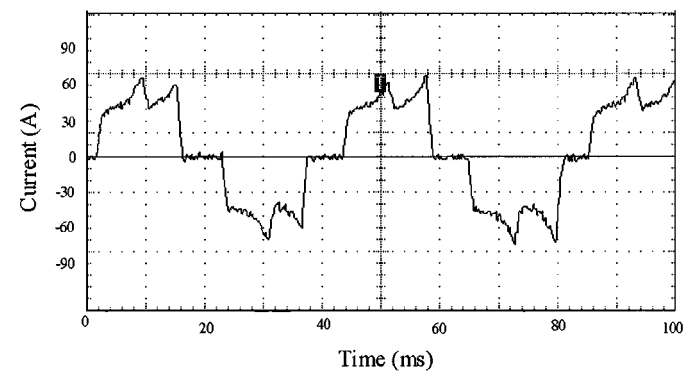Fig. 4.   Profile of the computed stator current.

Fig. 5.   Measured stator current.

IV. APPLICATION

A three phase-winding brushless d.c. motor (900 W / 24 V, 11 poles, 24 stator slots, 136 rpm, using Nd–Fe–B as excitation) is used as a typical example to demonstrate the proposed method. The motor is driven by a converter with two-phase-on excitation. In the multi-slice FEM the motor is divided into six slices and at each slice the mesh has 6654 nodes with 8912 elements. The time step size is 75 μs. The computed steady-state flux distribution is shown in Fig. 3. The computed and measured stator currents when the motor is fed with PWM voltages are shown in Figs. 4 and 5, respectively. The profile of the computed eddy-current loss in the PM is shown in Fig. 6. The averages of the eddy-current loss in the PM and the iron loss are 11.94 W and 20.95 W, respectively. The computed results show that the eddy-current loss in the PM is mainly caused by the commutation of the currents in stator windings.
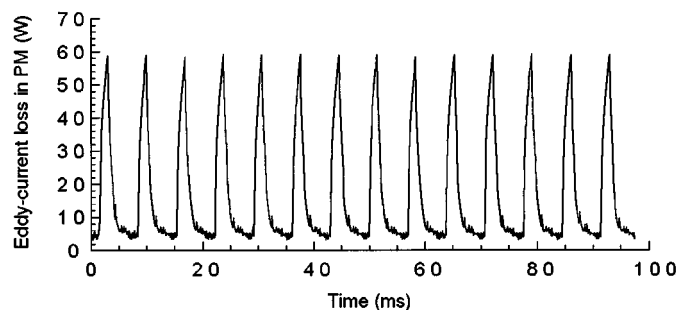
Fig. 6. Profile of the computed eddy-current loss in PM.

V. Conclusion

For studying the performance of brushless d.c. motors, the multi-slice FEM representing the PM in a network can include the effect of eddy-currents in the PM. The control loop is involved by coupling the stator circuit equations in the FEM whereas the impressed terminal voltages are governed by the controller. The solution can also include the effects of saturation, the relative movement of teeth and slots, the free wheeling diodes as well as the other nonsinusoidal quantities. The computed results show that the eddy-current loss in rare-earth PM should not be ignored in the loss estimation.

References

[1] F. Deng, "Commutation-caused eddy-current losses in permanent-magnet brushless dc motors," *IEEE Trans. Magn.*, vol. 33, no. 5, pp. 4310–4318, Sept. 1997.

[2] H. Polinder and M. J. Hoeijmakers, "Eddy-current losses in the segmented surface-mounted magnets of a PM machine," *IEE Proc.-Electr. Power Appl.*, vol. 146, no. 3, pp. 261–266, May 1999.

[3] M. S. N. Al-Din, A. F. Kader, and J. Al-Samarai, "A new method to compute eddy current losses by the finite elements method," in *IEEE Industry Applications Society Annual Meeting*, 1997, pp. 3–9.

[4] A. Boglietti, M. Chiampi, D. Chiarabaglio, and M. Tartaglia, "Finite element analysis of permanent magnet motors," *IEEE Trans. Magn.*, vol. 25, no. 5, pp. 3584–3586, Sept. 1989.

[5] Y. P. Liu, D. Howe, T. S. Birch, and D. M. H. Matthews, "Dynamic modeling and performance prediction of brushless permanent magnetic drive systems," in *Fourth International Conference on Electrical Machines and Drives*, 1989, pp. 95–99.

[6] F. Deng and N. A. Demerdash, "Comprehensive salient-pole synchronous machine parametric design analysis using time-step finite element-state space modeling techniques," *IEEE Trans. Energy Conversion*, vol. 13, no. 3, pp. 221–229, Sept. 1998.

[7] S. L. Ho, H. L. Li, and W. N. Fu, "Inclusion of inter-bar currents in a network-field coupled time stepping finite element model of skewed rotor induction motors," *IEEE Trans. Magn.*, vol. 35, no. 5, pp. 4218–4225, Sept. 1999.

[8] S. L. Ho, H. L. Li, W. N. Fu, and H. C. Wong, "A novel approach to circuit-field-torque coupled time stepping finite element modeling of electric machines," *IEEE Trans. Magn.*, vol. 36, pp. 1886–1889, 2000.

[9] S. L. Ho, W. N. Fu, and H. C. Wong, "Estimation of stray losses of skewed induction motors using coupled 2-D and 3-D time stepping finite element methods," *IEEE Trans. Magn.*, vol. 34, no. 5, pp. 3102–3105, 1998.